STUDIA UBB CHEMIA, LXVII, 2, 2022 (p. 193-203)
(RECOMMENDED CITATION)
DOI:10.24193/subbchem.2022.2.12

HALOGEN-BONDED SUPRAMOLECULAR ARCHITECTURES INVOLVING 2,7-DIPYRIDYLFLUORENE AND 1,3,5-TRIFLUORO-2,4,6-TRIIODOBENZENE TECTONS – A SPECTACULAR EVOLUTION FROM CATEMERS TO 2D HALOGEN BOND ORGANIC FRAMEWORKS (XBOF)

LIDIA CĂTA[a], IOANA GEORGETA GROSU[b], MARIA MICLĂUŞ[b], NICULINA DANIELA HĂDADE[a], ION GROSU[a] and ANAMARIA TEREC[a,*]

ABSTRACT. A spectacular 2D Halogen Bond Organic Framework (XBOF) was prepared by the mechanochemical solvent-drop grinding method (SCD) starting from 2,7-dipyridylfluorene and 1,3,5-trifluoro-2,4,6-triiodobenzene tectons. The formation of the supramolecular assembly was proved by powder X-ray diffraction measurements and the structural details were collected from the single crystal X-ray diffraction investigations.

Keywords: *N···I and I···F halogen bonds, XBOFs, dipyridylfluorene, 1,3,5-trifluoro-2,4,6-triiodobenzene, single crystal X-ray diffraction structure*

INTRODUCTION

The literature data reveal exciting supramolecular host-guest complexes involving macrocycles, [1] cryptands, [1a, 1b, 2] cages [1a, 1b, 3] or mechanically interlocked systems (e.g. rotaxanes or catenanes).[4] The fascinating world of supramolecular architectures was enriched by spectacular self-assembly processes of single molecules [5] or by self-sorting and directed assembly of complementary molecules having as driving forces hydrogen [6] or halogen bonds, [7] hydrophobic contacts, [8] charge transfer complexes [9] and cation- [1a, 1b, 10] or anion-organic [1b, 11] interactions.

[a] *Babes-Bolyai University, Faculty of Chemistry and Chemical Engineering, Department of Chemistry and SOOMCC, Cluj-Napoca, 11 Arany Janos, 400028, Cluj-Napoca, Romania*
[b] *National Institute for Research and Development of Isotopic and Molecular Technologies, 67-103 Donath str., RO-400293, Cluj-Napoca, Romania*
** Corresponding author: anamaria.terec@ubbcluj.ro*

Halogen bonds [12] proved to be versatile tools in supramolecular chemistry. The obtaining of pure organic supramolecular structures by the cocrystallisation (supramolecular synthesis) of polydentate halogen donors and halogen acceptors lead to outstanding XBOFs [Halogen(X) Bond Organic Frameworks; 1D, [7c, 13] 2D [14] or 3D [7d, 15] polymeric structures].

In a previous work we investigated the N···I halogen bond-based formation of catemers using 2,7-dipyridylfluorene (2,7-DPF) **1** as halogen acceptor and *ortho*-, *meta*- and *para*-diiodo-tetrafluorobenzene (DITFB) isomers (**2**–**4**; Figure 1) as halogen donors. [7c] The single crystal X-ray diffraction structures of these 1D polymers (catemers I-III) revealed a significant correlation between the structures of the polymers and the geometries of the halogen donors (Figure 2).

In this context we considered of interest to develop N···I halogen bond-based 2D networks (XBOFs) using 2,7-DPF (**1**) as ditopic halogen acceptor and 1,3,5-trifluoro-2,4,6-triiodobenzene (**5**, TFTIB) as tritopic halogen donor (Figure 3).

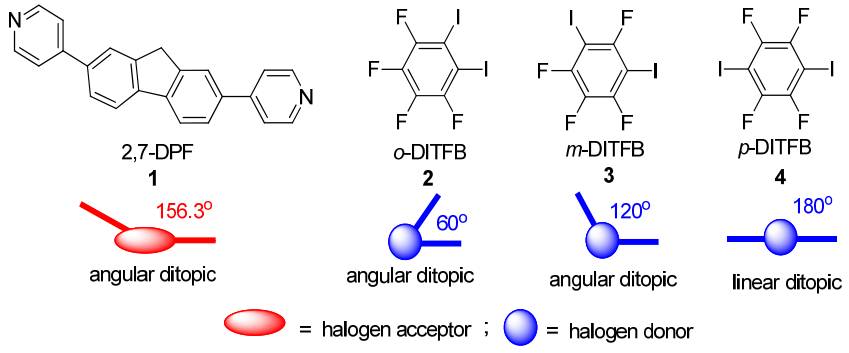

Figure 1. Halogen donors and acceptors used for the access to 1D polymers by N···I contacts

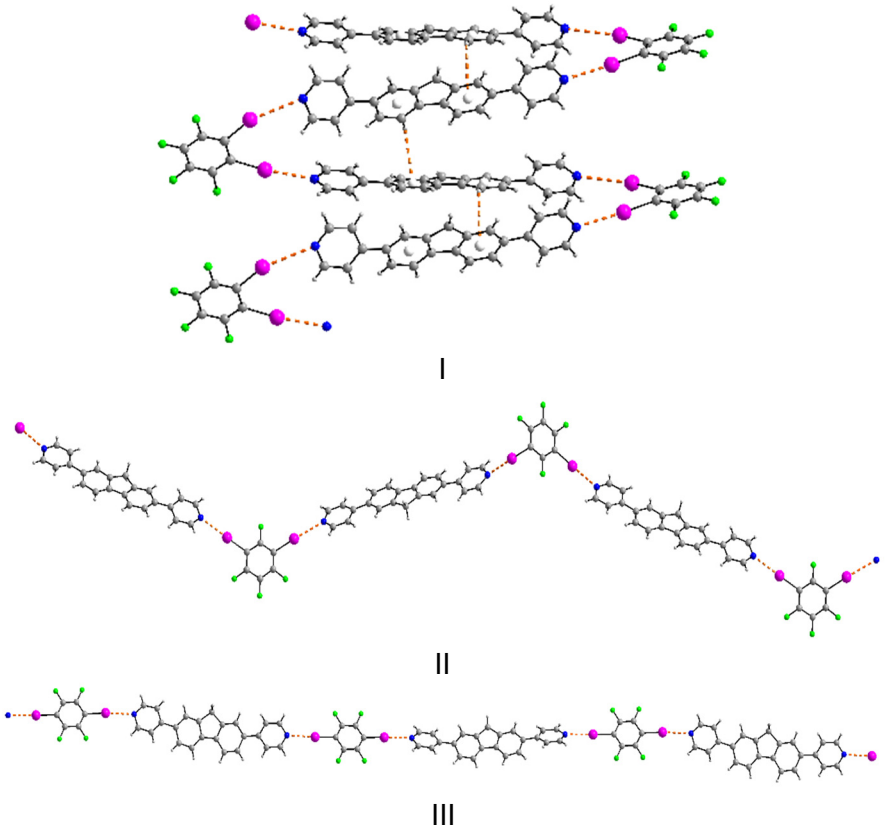

Figure 2. N···I halogen bond catemers with angular (I and II) and linear (III) geometries

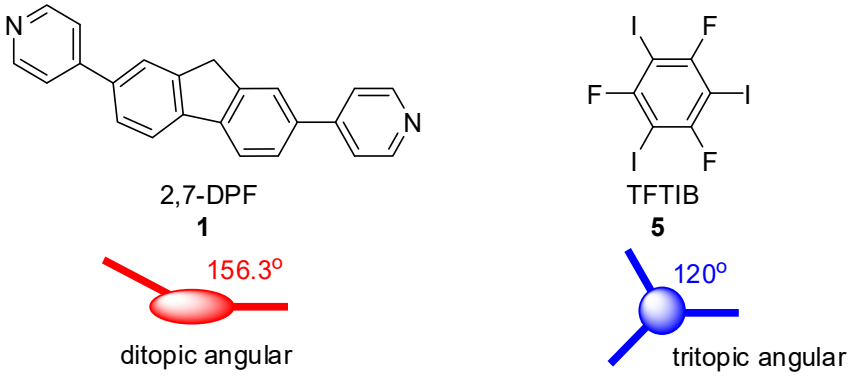

Figure 3. Proposed halogen acceptor (**1**) and halogen donor (**5**) for the access to 2D Halogen Bond Organic Frameworks (XBOFs)

RESULTS AND DISCUSSIONS

The halogen bond-based supramolecular architecture **(2,7-DPF)(TFTIB)** was obtained by the mechanochemical solvent-drop grinding method (SDG) [16] using a Retsch MM400 mixer mill (120 min at 30 Hz) with stainless steel grinding jars (1.5 mL). 2,7-Dipyridylfluorene (**1**; 0.06 mmol) and 1,3,5-trifluoro-2,4,6-triiodobenzene (**5**; 0.04 mmol) were used in stoichiometric amounts (Scheme 1). Small amount (50 μL) of chloroform was added as solvent.

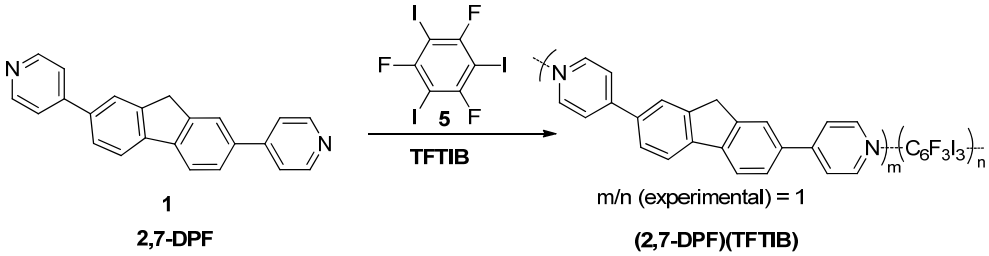

Scheme 1

The formation of the self-assembled entities was monitored by powder X-ray diffractometry (Figure 4). Single crystals suitable for the molecular structure determination were obtained by slow evaporation of the solvent from a $CHCl_3$ solution of **(2,7-DPF)(TFTIB)**. Surprisingly, in the crystal, an experimental ratio of 2,7-DPF / TFTIB = 1 was observed instead of the expected 2,7-DPF / TFTIB = 3 / 2 ratio. The equimolecular ratio of halogen

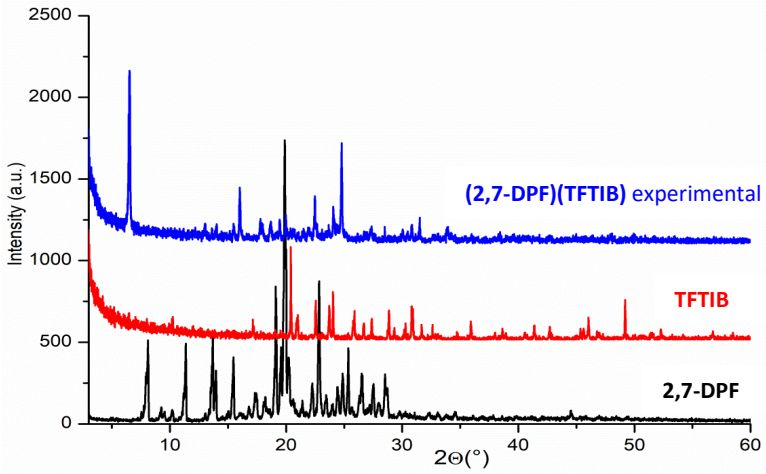

Figure 4. Powder X-ray diffraction spectra of compound 2,7-DPF (bottom), TFTIB (middle) and **(2,7-DPF)(TFTIB)** (top)

donors and acceptors was confirmed using powder X-ray diffractometry for the bulk powder, too. The experimental spectrum (of the raw product) and the theoretical one (calculated from the single crystal X-ray diffraction measurements) (Figure 5) were similar and proved the presence of the same structures in the bulk powder product and in the measured crystal.

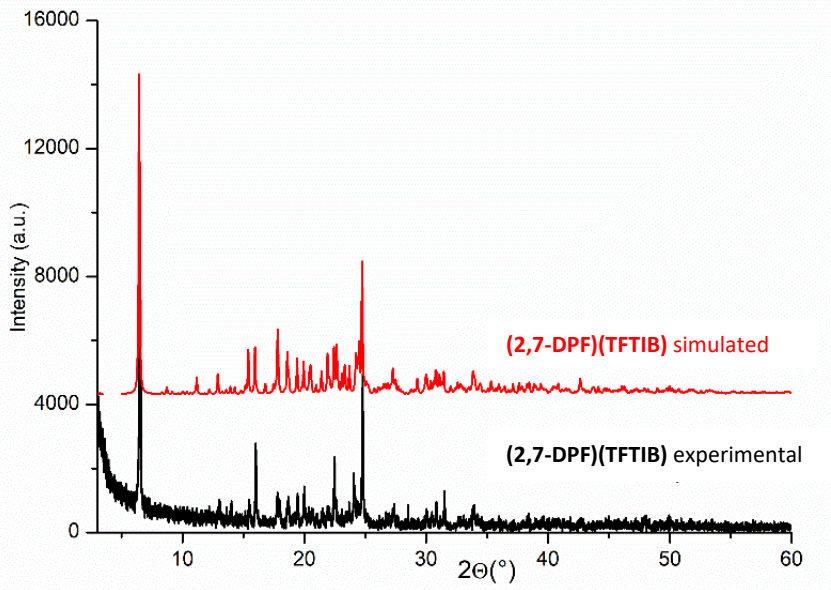

Figure 5. Experimental (bottom) and simulated (top) powder X-ray diffraction spectra of cocrystal **(2,7-DPF)(TFTIB)**

The repetitive unit in the single crystal X-ray diffraction structure of **(2,7-DPF)(TFTIB)** shows two geometries for the 2,7-DPF units connected to the TFTIB moieties, unit A and unit B (Figure 6a). The fluorene units are slightly curved, with a dihedral angle between the benzene rings of 7.1° (unit A) and 5.8° (unit B), respectively. Interestingly, the pyridine moieties exhibit quite different torsion angles with the adjacent benzene rings in the two units: 13.45° and 32.36° in unit B, and very close values for the torsion angles in unit A, 26.82° and 31.15°, respectively, bringing the pyridyl units almost coplanar to each other in the latter case, with consequences in their different association pattern as mentioned further.

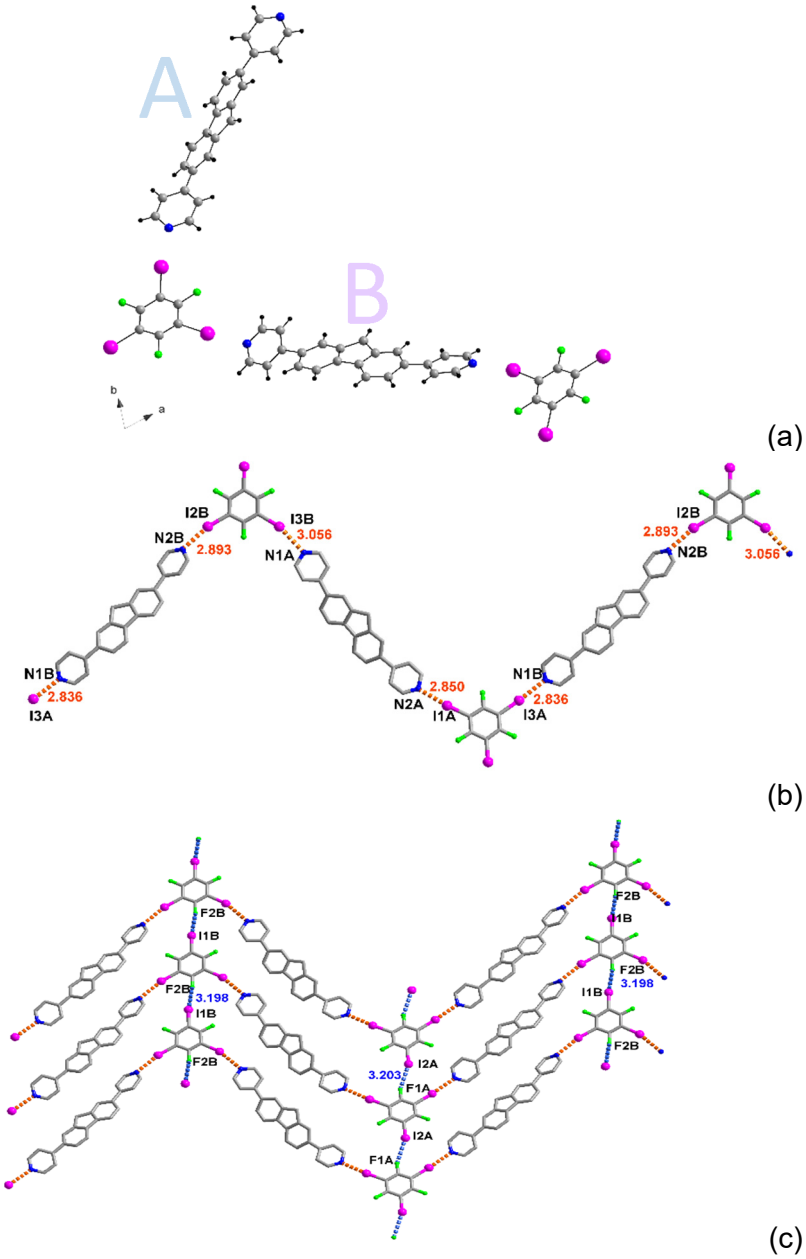

Figure 6. Halogen bonding motifs in the single crystal X-ray structure of **(2,7-DPF)(TFTIB)** cocrystal: repetitive unit (A and B units) (a); I···N (orange) generated catemer (b); 2D sheet *via* additional I···F contacts (blue) (c).

The thus determined structure of the cocrystal was found to contain halogen-bonded 2,7-DPF and TFTIB molecules. The 2,7-DPF is participating in halogen bonding with the nitrogen acceptor atoms, while TFTIB acts as a ditopic halogen donor in this arrangement as only two of its iodine atoms are involved in I···N halogen bonding, most probably due to steric impediments, resulting into zig-zag infinite supramolecular chains (Figure 6b). The TFTIB moiety is involved further *via* its third iodine atom in I···F contacts that lead to the formation of a quasi-coplanar 2D sheet, parallel to the crystallographic *a* axis (Figure 6c). In order to assess the strength of the formed halogen bonds, the relative shortenings of the I···Acceptor bonds were calculated and are included in Table 1 alongside the values for the halogen bond length and C–I···Acceptor angles.

Table 1. Halogen bond length (*d*), Angle, Relative Shortening (*R.S.)* of I···Acceptor distances in **(2,7-DPF)(TFTIB)** cocrystal

I···Acceptor	*d*(I···Acceptor)/Å	*R.S.*‡/%	Angle (C–I···Acceptor)/°
I1A···N2A	2.85	19.26	172.19
I3A···N1B	2.836	19.66	176.07
I2B···N2B	2.893	18.05	167.77
I3B···N1A	3.056	13.43	164.44
I2A···F1A	3.203	7.16	160.95
I1B···F2B	3.198	7.3	163.44

‡ *R.S.* was calculated as $R.S. = \{1 - d(\text{I}\cdots\text{Acceptor})/[r_{vdW}(\text{I}) + r_{vdW}(\text{Acceptor})]\}*100$

As observed in Table 1, the nitrogen atoms form quite strong halogen bonds, 18-19.66% shorter than the sum of the van der Waals radii in most cases and the bond angles are acceptable. The I···F bonds are less shortened, but in good agreement with other similar assemblies [14d] and contribute to the overall stability of the structure.

The 2D sheets stack further into layers *via* reciprocal C-H···aromatic contacts between H atoms pertaining to the pyridine rings in one sheet and the phenyl ring of the fluorene in the next sheet ($d_{C(23B)–H\cdots centroid\ Ph}$ = 3.153 Å) and moreover interconnected by C-H···F hydrogen-bonding contacts ($d_{C(3B)–H\cdots F1B}$ = 3.207 Å) with a shifted TFTIB unit underneath into a complex 3D architecture (Figure 7). It is interesting to mention that only unit B of 2,7-DPF is involved in such short contacts, while for unit A only significantly larger contact values were observed.

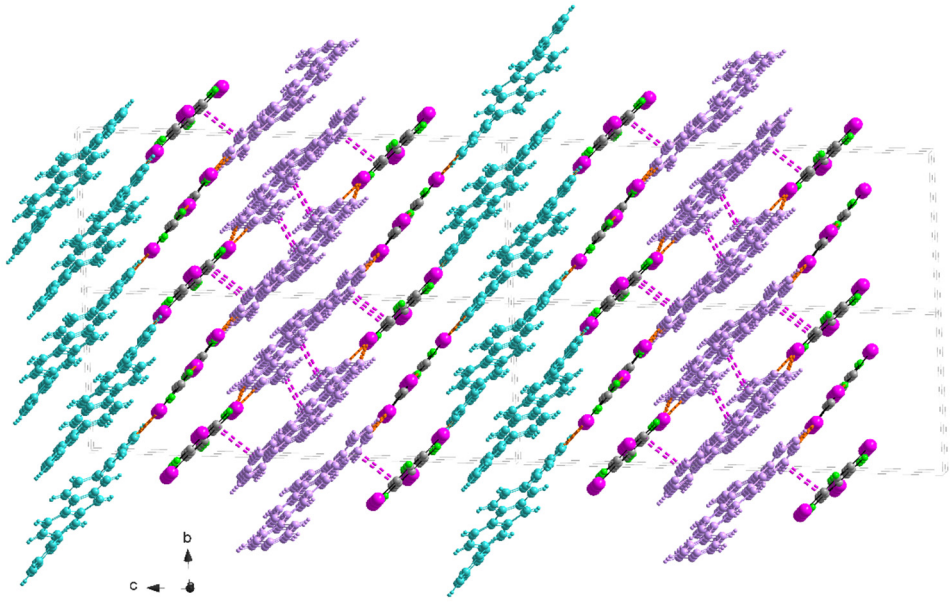

Figure 7. Double layers interconnected by C–H···aromatic and C–H···F contacts (violet) in **(2,7-DPF)(TFTIB)** – A units are represented in aqua, B units in pink

CONCLUSIONS

Ditopic halogen acceptor 2,7-DPF and tritopic halogen donor TFTIB form a 2D halogen bond organic framework (XBOF) by N···I and I···F contacts. The sheets are connected in a 3D structure by C–H···aromatic and C–H···F interactions. The TFTIB molecules form catemers by I···F contacts and thus, only two iodine atoms of the donor molecules are involved in N···I contacts. The competition between I···N and I···F halogen bonds determines the peculiar supramolecular structure of **(2,7-DPF)(TFTIB)** co-crystal and the unexpected 2,7-DPF / TFTIB equimolecular ratio in the crystals.

EXPERIMENTAL PART

General data for X-ray diffraction measurements for **(2,7-DPF)(TFTIB)**

X-ray Powder Diffraction (XRPD)

X-ray patterns were collected at room temperature with a Rigaku Smart Lab multipurpose diffractometer, using Cu Kα1 radiation (λ= 1.54056 Å), equipped with a 9 kW rotating anode. For the acquisition of the experimental

data Smart Lab Guidance software were used. The samples were ground to a fine homogeneous powder using an agate pestle and mortar and mounted in a sample holder. The measurements were performed in the 3–60˚ range in steps of 0.01˚.

Single-crystal X-ray diffraction measurement

Single-crystal diffraction data were collected, at room temperature, on an Oxford Diffraction SuperNova dual wavelength diffractometer with operating mirror monochromated MoK*α* radiation mode (λ = 0.71073 Å). X-ray data collection was monitored and all the data were corrected for Lorentzian, polarization and absorption effects using CrysAlisPro program [Agilent Technologies, CrysAlis PRO, Yarnton Oxfordshire, England: Agilent Technologies, 2010] Olex2 program was used for the crystal structures solution and refinement, [17] SHELXT was used for structures solutions and for full matrix least-squares refinement on F2 (Table 2). [18]

Table 2. Crystallographic data for **(2,7-DPF)(TFTIB)**

Identification code		**(2,7-DPF)(TFTIB)**	
Empirical formula	$C_{58}H_{30}F_6I_6N_4$	γ/°	72.835(4)
Formula weight	1658.30	Volume	2695.4(2) $Å^3$
Wavelenght	1.54184	Z	2
Temperature	293(2) K	Density (calculated)	2.043 g/cm^3
Crystal system	triclinic	Absorption coefficient mm^{-1}	27.685
Space group	P-1	F(000)	1556.0
a/Å	9.2485(3)	Reflections collected	17255
b/Å	11.1194(6)	Data/restraints/parameters	9965 /2/667
c/Å	27.5846(9)	Goodness-of-fit on F^2	1.104
α/°	84.698(3)	Final R indexes [I>=2σ (I)]	R_1 = 0.1048, wR_2 = 0.2715
β/°	85.714(3)	Final R indexes [all data]	R_1 = 0.1333, wR_2 = 0.3333
		Largest diff. peak/hole / e $Å^{-3}$	2.82/-1.72

The structural data were deposited at Cambridge Crystallographic Data Center (number CCDC 2180363).

ACKNOWLEDGEMENTS

We are grateful for the financial support of this work by CNCS-UEFISCDI, project PN-III-P4-ID-PCCF-2016-0088.

REFERENCES

[1] a) J.-M. Lehn, *Supramolecular chemistry: concepts and perspectives*; VCH, Weinheim, **1995**; b) J. W. Steed, J. L. Atwood, *Supramolecular Chemistry*, Wiley, New York, **2009**; c) Lehn, J.-M., *Angew. Chem. Int. Ed*. **2015**, *54*, 3276 – 3289; d) D. Qiao, H. Joshi, H. Zhu, F. Wang, Y. Xu, J. Gao, F. Huang, A. Aksimentiev, J. Feng, *J. Am. Chem. Soc*. **2021**, *143*, 15975−15983; e) J. Wang, Y.-Y. Ju, K.-H. Low, Y.-Z. Tan, J. Liu, *Angew. Chem. Int. Ed*. **2021**, *60*, 11814 – 11818; f) M. Balog, I. Grosu, G. Plé, Y.Ramondenc, E. Condamine, R. Varga, *J. Org. Chem.* **2004***, 69,* 1337-1345.

[2] a) S. Sarkar, P. Sarkar, P. Ghosh, *J. Org. Chem*. **2021**, *86*, 6648−6664; b) C. V. Crişan, A. Soran, A. Bende, N. D. Hădade, A. Terec, I. Grosu, *Molecules,* **2020**, *25*, nr. 3789; c) C.V. Crişan, A. Terec, N. D. Hădade, I. Grosu, *Tetrahedron*, **2015**, *71*, 6888-6893.

[3] a) W. Wang, Y.-X. Wang, H.-B. Yang, *Chem. Soc. Rev.* **2016**, *45,* 2656–2693; b) G. Liu, M. Zeller, K. Su, J. Pang, Z. Ju, D. Yuan, M. Hong, *Chem. Eur. J*. **2016**, *22*, 17345 – 17350; c) S. Wang, T. Sawada, K. Ohara, K. Yamaguchi, M. Fujita, *Angew. Chem. Int. Ed*. **2016**, *55*, 2063 –2066.

[4] a) J. E. M. Lewis, M. Galli, S. M. Goldup, *Chem. Commun.* **2017**, *53*, 298—312; b) N. Pearce, M. Tarnowska, N. J. Andersen, A. Wahrhaftig-Lewis, B. S. Pilgrim, N. R. Champness, *Chem. Sci*., **2022**, *13*, 3915–3941; c) C.-Y. Chen, H.-C. Xu, T.-H. Ho, C.-J. Hsu, C.-C. Lai, Y.-H. Liu, S.-M. Peng, S.-H. Chiu, *J. Org. Chem*. **2021**, *86*, 13491−13502.

[5] a) I. Hisaki, *J. Incl. Phenom. Macrocycl. Chem*. **2020**, *96*, 215–231; b) P. Li, P. Li, M. R. Ryder, Z. Liu, C. L. Stern, O. K. Farha, J. F. Stoddart *Angew. Chem. Int. Ed*. **2019**, *58*, 1664 – 1669; c) R.-B. Lin, Y. He, P. Li, H. Wang, W. Zhou, B. Chen, *Chem. Soc. Rev*. **2019**, *48*, 1362-1389; d) T. Adachi, M.D. Ward, *Acc. Chem. Res*. **2016**, *49*, 2669 – 2679; e) Y.-L. Li, E. V. Alexandrov, Q. Yin, L. Li, Z.-B. Fang, W. Yuan, D. M. Proserpio, T.-F. Liu, *J. Am. Chem. Soc*. **2020**, *142*, 7218−7224; f) M. Circu, V. Pascanu, A. Soran, B. Braun, A. Terec, C. Socaci, I. Grosu, *CrystEngComm,* **2012,** *14,* 632-639.

[6] a) Y. Feng, D. Philp, *J. Am. Chem. Soc*. **2021**, *143*, 17029−17039; b) Y. Liu, J. Dai, Z. Zhang, Y. Yang, Q. Yang, Q. Ren, Z. Bao, *Chem Asian J.* **2021**, *16*, 3978–3984; c) I. Hisaki, C. Xin, K. Takahashi, T. Nakamura, *Angew. Chem. Int. Ed*. **2019**, *58*, 11160 – 11170; d) S. A. Boer, M. Morshedi, A. Tarzia, C. J. Doonan, N. G. White, *Chem. Eur. J.* **2019**, *25*, 10006 – 10012; e) L. Pop, N. D. Hădade, A. van der Lee, M. Bărboiu, I. Grosu, Y.-M. Legrand, *Cryst. Growth Des.*, **2016**, *16*, 3271–3278.

[7] a) L. Sun, W. Zhu, X. Zhang, L. Li, H. Dong, W. Hu, *J. Am. Chem. Soc*. **2021**, *143*, 19243−19256; b) G. Gong, S. Lv, J. Han, F. Xie, Q. Li, N. Xia, W. Zeng, Y. Chen, L. Wang, J. Wang, S. Chen, *Angew. Chem. Int. Ed*. **2021**, *60*, 14831 –14835; c) I. G. Grosu, L. Pop, M. Miclăuş, N. D. Hădade, A. Terec, A. Bende, C. Socaci, M. Bărboiu, I. Grosu, *Cryst. Growth Des.,* **2020***, 20*, 3429-3441; d) L. Pop, I. G. Grosu, M. Miclăuş, N. D. Hădade, A. Pop, A. Bende, A. Terec, M. Barboiu, I. Grosu, *Cryst. Growth Des.,* **2021***, 21*, 1045-1054; e) M. Miclăuş, X. Filip, C. Filip, F. Martin, I. G. Grosu, *J. Pharm. Biomed. Anal.* **2016**, *124,* 274-280.

[8] a) F. Biedermann, W. M. Nau, H.-J. Schneider, *Angew. Chem., Int. Ed*. **2014**, *53*, 11158−11171; b) J. H. Jordan, B. C. Gibb, *Chem. Soc. Rev*. **2015**, *44*, 547−585; c) L. Pop, F. Dumitru, N. D. Hădade, Y.-M. Legrand, A. van der Lee, M. Bărboiu, I. Grosu, *Org. Lett.* **2015**, *17*, 3494−3497.

[9] a) H. Su, S. A. H. Jansen, T. Schnitzer, E. Weyandt, A. T. Rösch, J. Liu, G. Vantomme, E. W. Meijer, *J. Am. Chem. Soc*. **2021**, *143*, 17128−17135; b) J. Hwang, P. Li, K. D. Shimizu, *Org. Biomol. Chem*. **2017**, *15*, 1554−1564; c) A. Das, S. Ghosh, *Angew. Chem., Int. Ed*. **2014**, *53*, 2038−2054.

[10] a) S. Yang, A. Miyachi, T. Matsuno, H. Muto, H. Sasakawa, K. Ikemoto, H. Isobe *J. Am. Chem. Soc*. **2021**, *143*, 15017−15021; b) D. Preston, *Angew. Chem. Int. Ed.* **2021**, *60*, 20027 – 20035; c) J. Shi, M. Wang, *Chem Asian J.* **2021**, *16*, 4037–4048.

[11] a) I. G. Grosu, M. I. Rednic, M. Miclăuş, I. Grosu, A. Bende, *Phys. Chem. Chem. Phys*. **2017**, *19*, 20691-20698; b) M. I. Rednic, R. A. Varga, A. Bende, I. G. Grosu, M. Miclăuş, N. D. Hădade, A. Terec, E. Bogdan, I. Grosu, *Chem. Commun.*, **2016**, *52*, 12322-12325.

[12] a) D. M. P. Mingos, Series Editor for *Structure and Bonding*, Metrangolo, P; Resnati, G; editors for volume 126: *Halogen Bonding – Fundamentals and Applications*, Springer, Berlin, **2008**, volume 126; b) P. Metrangolo, G. Resnati, editors, *Halogen Bonding II, Impact on the Materials Chemistry and Life Sciences*, *Topics in Current Chemistry*, Springer, Berlin, **2015**, volume 359; c) P. M. J. Szell, S. Zablotny, D. L. Bryce, *Nat. Commun*. **2019**, Article number: 916; d) G. Cavallo, P. Metrangolo, R. Milani, T. Pilati, A. Priimagi, G. Resnati, G. Terraneo, *Chem. Rev*. **2016**, *116*, 2478 – 2601.

[13] a) M. C. Pfrunder, A. S. Micallef, L. Rintoul, D. P. Arnold, K. J. P. Davy, J. McMurtrie, *Cryst. Growth Des*. **2014**, *14*, 6041−6047; b) V. I. Nikolayenko, D. C. Castell, D. P. van Heerden, L. J. Barbour, *Angew. Chem., Int. Ed*. **2018**, *57*, 12086−12091; c) D. Bulfield, E. Engelage, L. Mancheski, J. Stoesser, S. M. Huber, *Chem. Eur. J*. **2020**, *26*, 1567−1575.

[14] a) N. Biot, D. Bonifazi, *Chem. Eur. J.* **2020**, *26*, 2904−2913; b) M. Su, X. Yan, X. Guo, Q. Li, Y. Zhang, C. Li, *Chem. Eur. J.* **2020**, *26*, 4505−4509; c) M.-P. Zhuo, Y.-C. Tao, X.-D. Wang, Y. Wu, S. Chen, L.-S. Liao, L. Jiang, *Angew. Chem. Int. Ed.* **2018**, *57*, 11300−11304; d) N. Baus Topić, N. Bedeković, K. Lisac, V. Stilinović, D. Cinčić, *Cryst. Growth Des.* **2022**, *22*, 3981-3989.

[15] a) S. Shankar, O. Chovnik, L. Shimon, M. Lahav, M. E. van der Boom, *Cryst. Growth Des*. **2018,** *18*, 1967−1977; b) N. Chongboriboon, K. Samakun, T. Inprasit, F. Kielar, W. Dungkaew, L. W.-Y. Wong, H. H.-Y. Sung, D. B. Ninkovic, S. D. Zaric, K. Chainok, *CrystEngComm* **2020**, *22*, 24−34; c) K. Raatikainen, K. Rissanen, *CrystEngComm* **2011**, *13*, 6972−6977.

[16] a) J. L. Howard, Q. Cao, D. L. Browne, *Chem. Sci*. **2018**, *9*, 3080−3094; b) M. Leonardi, M. Villacampa, J. C. Menéndez, *Chem. Sci*. **2018**, *9*, 2042−2064; c) M. Obst, B. Konig, *Eur. J. Org. Chem*. **2018**, 4213−4232.

[17] O. V. Dolomanov, L. J. Bourhis, R. J. Gildea, J. A. K. Howard, H. Puschmann, *J. Appl. Cryst*. **2009**, *42*, 339-341.

[18] G. M. Sheldrick, *Acta Cryst. A* **2015**, *71*, 3-8.